

SOME KINEMATICALLY ADMISSIBLE VELOCITY FIELDS IN MULTIMATERIAL EXTRUSION ⁽¹⁾

G. S. M I S H U R I S and R. E. Ś L I W A

RZESZÓW UNIVERSITY OF TECHNOLOGY

ul. W. Pola 2, 35-959, Rzeszów, Poland

Two different models of flow fields are proposed to describe plastic deformations during the extrusion of multi-metal composites. To construct the presented kinematically admissible flow fields, some information is adopted from experimental works concerning extrusion of longitudinally oriented metal composites. Formulae for velocities, strain-rate tensor and deviator of stresses are found.

1. INTRODUCTION

Metallic composite materials are heterogeneous materials consisting of two or more components bonded internally together; at least the largest component of that material (by volume) is a metal or an alloy. The type of spatial arrangement of components and their features decide on the flow behaviour of composite materials.

All these structures are composites of various degrees of complexity. A typical multimaterial consists of the core, a cylindrical body of one metal, which is surrounded by a concentric cylindrical sleeves of other metals.

There are numerous papers concerning such deformation in co-extrusion but relating rather to bimaterial (as the simplest multimetal) extrusion, e.g. [1 - 5, 7, 9, 10, 13], and containing analytical and experimental description of plastic flow of different metals. Most of the theoretical ones assume proportional flow, without taking into account the real behaviour of various metals deformed simultaneously. To approach the reality it is necessary to introduce true parameters of complex

¹Paper presented at the 2nd Seminar "Integrated Study on the Foundations of Plastic Deformation of Metals", at Dąbrówka (near Łańcut, Poland) Nov. 16 - 19, 1998

deformation. An example of such a procedure was presented in the papers [15 – 18, 20].

The results of papers e.g. [5, 6, 8, 11-14, 17, 18, 20 – 22] lead to determination of the character of flow and kinematically admissible velocity fields for the upper bound method, but only the works [17, 18, 20] follow to construct velocity fields for materials extruded simultaneously taking into account the results of their real behaviour.

Different mechanical behaviour of various metals and predicted deformation of components and composite were evaluated in special experimental test [15].

These tests (see Figs. 1 – 7) enable the evaluation of the actual tendency of different materials to undergo simultaneous plastic deformation (deformation of the components in comparison with the composite, determination of the limiting strain).

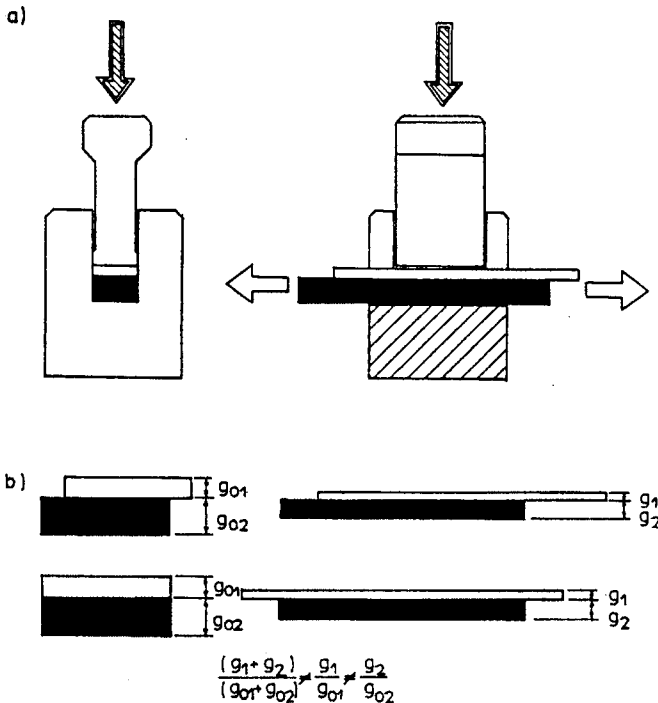
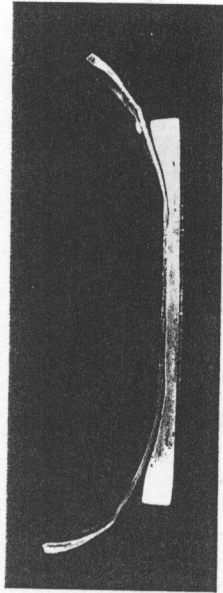
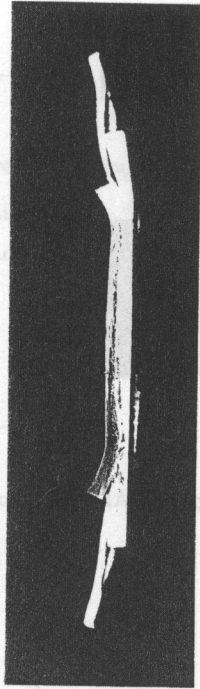


FIG. 1. Diagram of the test determining the extrudability of composed material: a) schematic process, b) composed specimens used in the test before and after simultaneous plastic deformation.

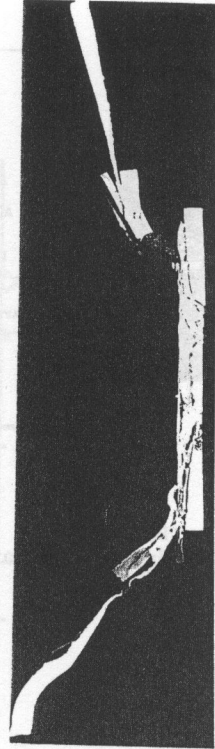
Basing on such information on simultaneous deformation of various materials, analysis of experimental results of co-extrusion and attempts to model the extrusion of sleeve-core systems [15 – 18], two models of extrusion of multimate-



a)



b)



c)

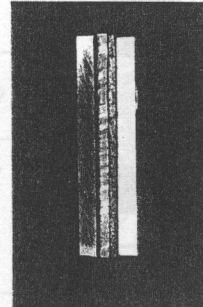
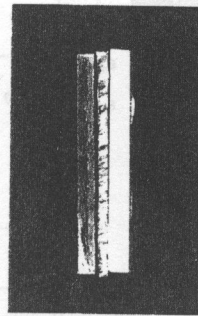


FIG. 2. Composed specimens used in the test before and after simultaneous plastic deformation:
 a) two components (from top to bottom - Pb/Al), b) three components (Al/OT3/Cu), c) four
 components (Cu/OT3/Cu/PA6N).

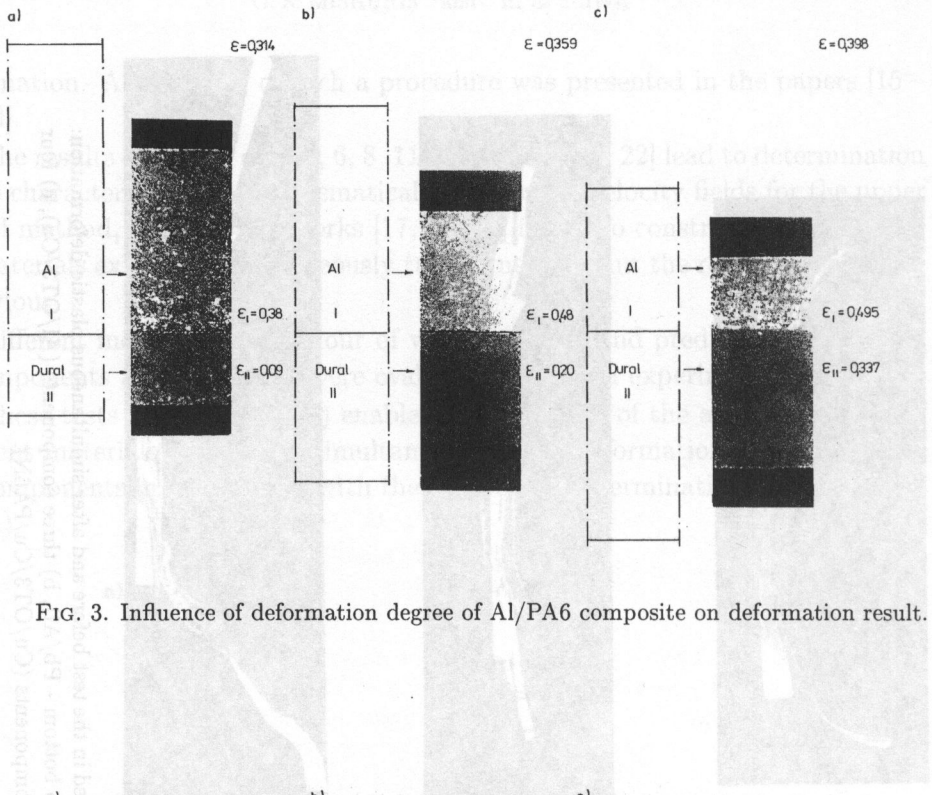


FIG. 3. Influence of deformation degree of Al/PA6 composite on deformation result.

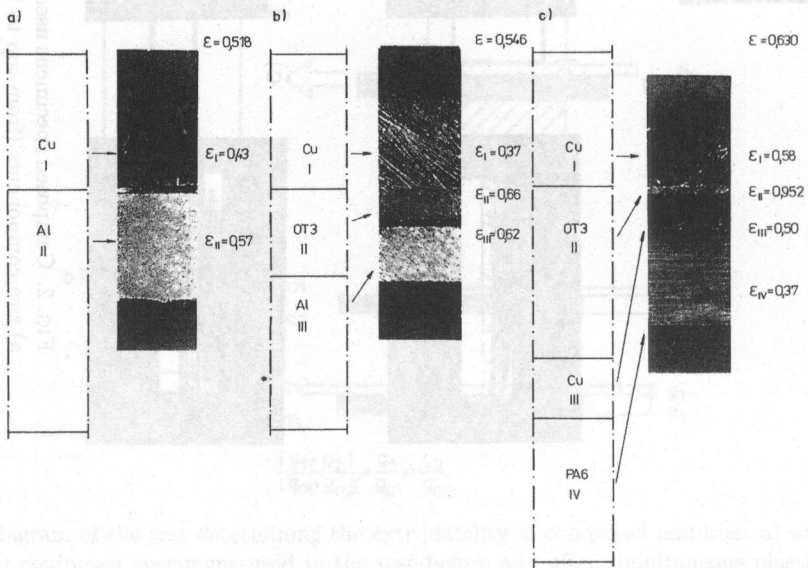


FIG. 4. Test results of the simultaneous plastic deformation of specimens: a) two materials, b) three materials, c) four materials.

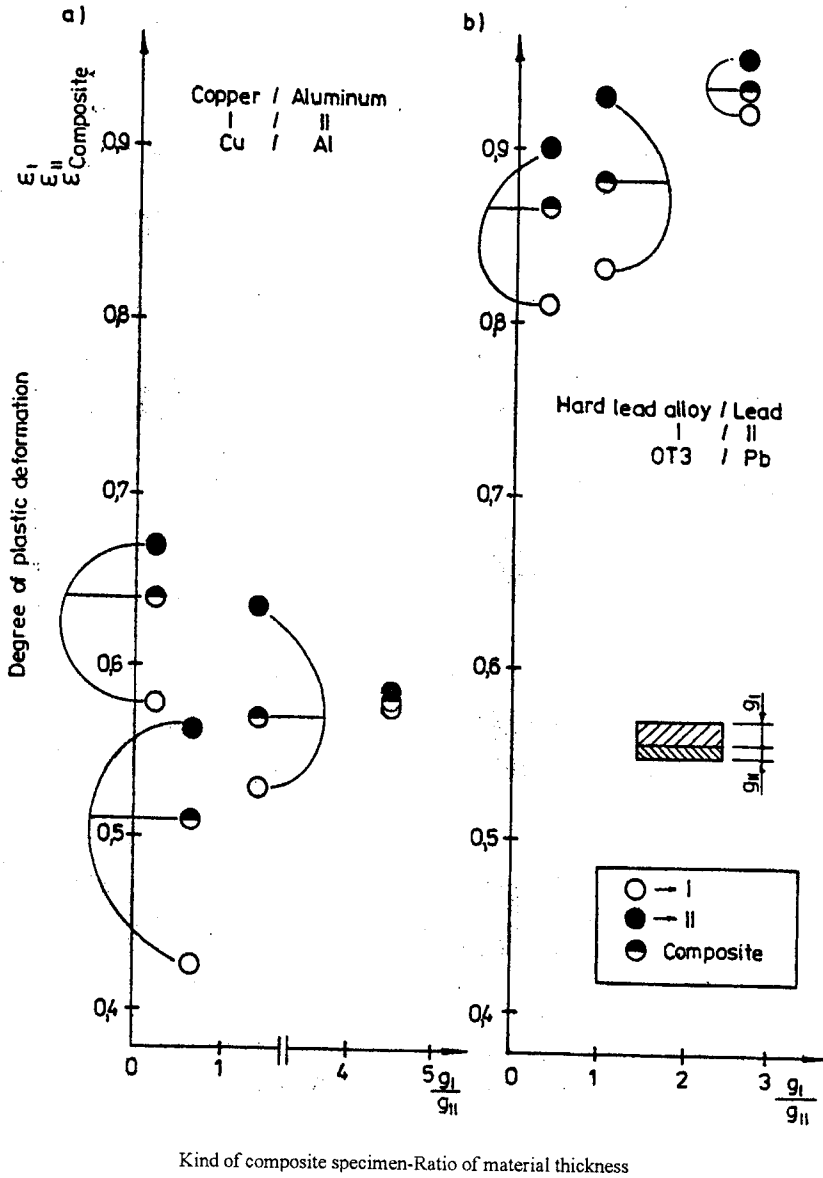


FIG. 5. Variation in the global and components' deformation degree ε , ε_I , ε_{II} for different cases of composites: a) Cu/Al, b) OT3/Pb.

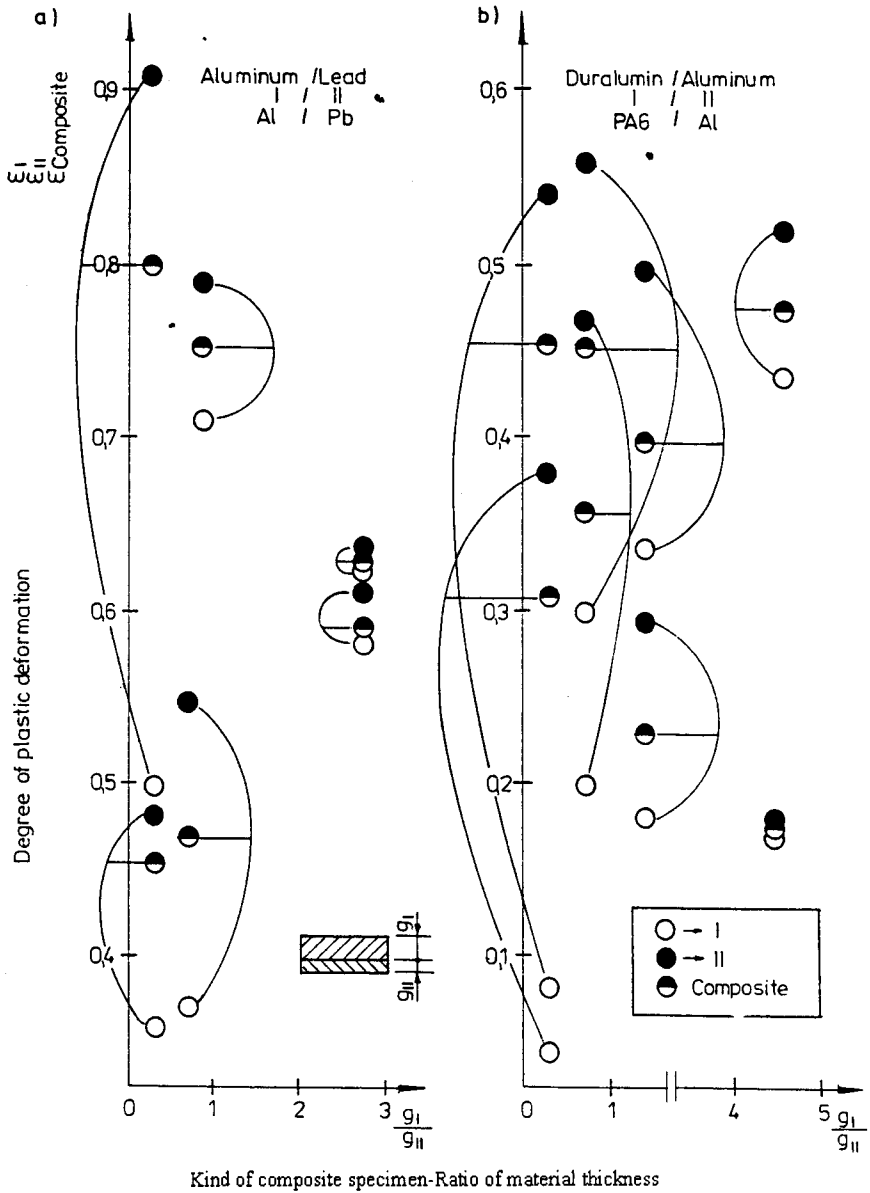


FIG. 6. Variation in the global and components' deformation degree $\epsilon, \epsilon_I, \epsilon_{II}$ for different cases of composites: a) Al/Pb, b) PA6/Al.

rial are presented. To construct the respective kinematically admissible velocity fields, the following assumptions are made [17, 18]:

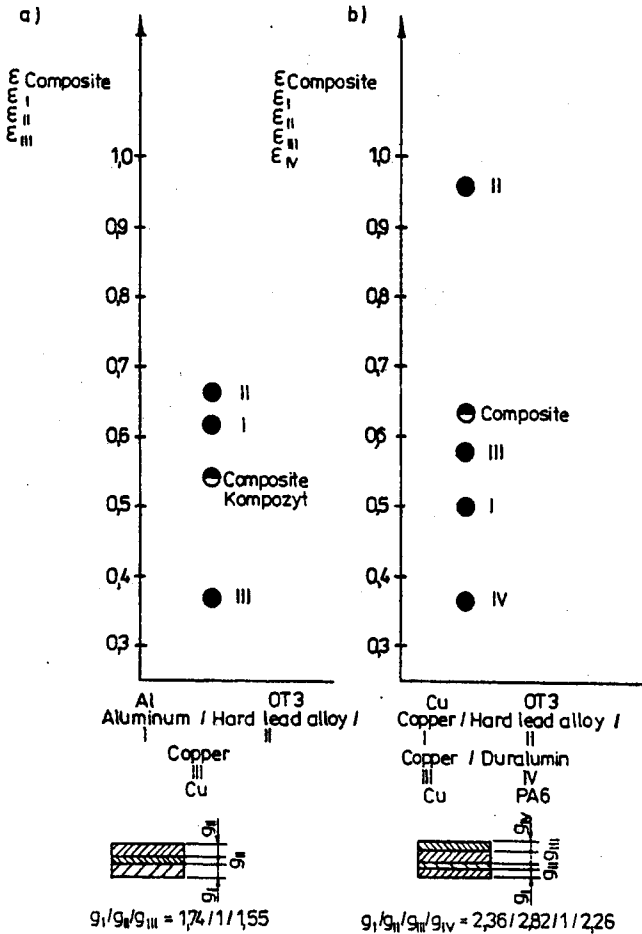


FIG. 7. Variation in the global and components' deformation degree ϵ , ϵ_I , ϵ_{II} for different cases of composites: a) Al/OT3/Cu, b) Cu/OT3/Cu/PA6.

- All materials of the core and the sleeves exhibit their own plastic regions described by boundaries $A_i A_{i+1} B_{i+1} B_i$, ($i = 0, \dots, n+1$), respectively (see Fig. 8).

The final degree of deformation is different for the core and all the sleeves:

$$(1.1) \quad \bar{\lambda}_0 = \frac{\bar{R}_0^2}{\underline{R}_0^2}, \quad \bar{\lambda}_j = \frac{\bar{R}_{j+1}^2 - \bar{R}_j^2}{\underline{R}_{j+1}^2 - \underline{R}_j^2}, \quad j = 1, \dots, n, \quad \bar{\lambda}_0 \neq \bar{\lambda}_j \neq \bar{\lambda}_{global}.$$

However, it is similar in each of the material components, so the exiting velocities of components are "constant" but not the same.

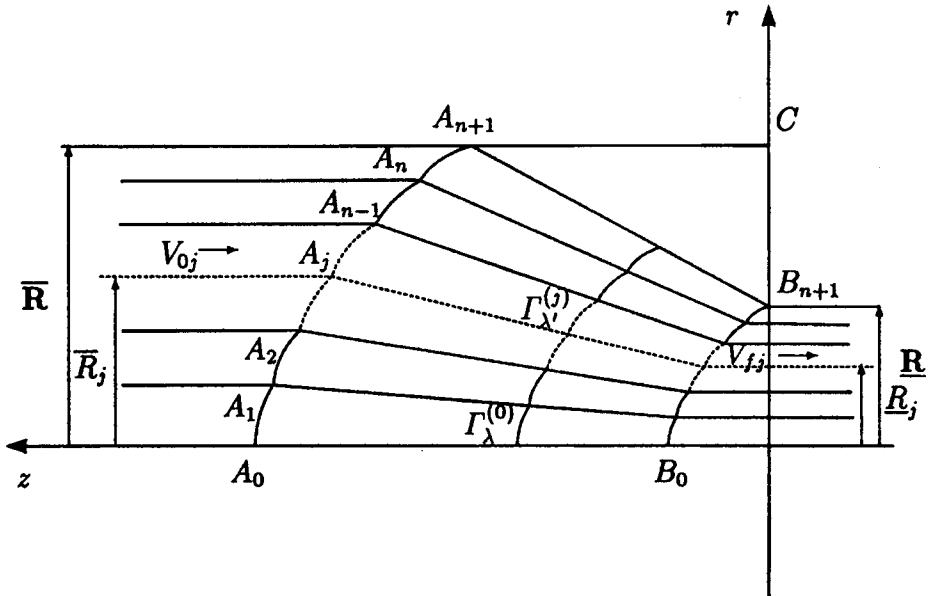


FIG. 8. Multi-metal extrusion under straight flow line hypothesis.

– During co-extrusion of the composite material by means of the flat die, the dead metal zone always exists. Its form depends on the geometry of extrusion tools and the properties of materials extruded.

– All materials are assumed to be incompressible.

– In general, velocities at the entry of the plastic zone have different values ($V_{0j} > 0$) for every component of the composite.

– Flow lines in the plastic zone are straight lines (Model 1) or special trigonometrical functions (Model 2) for the core and all the sleeves.

The object of this study is to define the kinematically admissible velocity fields in such type of multimetal extrusion, enabling the plastic flow of a rod composed of various metals to take place without fracture.

2. MODEL 1. STRAIGHT FLOW LINES IN THE PLASTIC ZONE

The results presented below are some extensions of those shown in [17] for bimaterial extrusion process on the case of multi-material extrusion.

Let us suppose for a moment that Cartesian coordinates (r, z) of the points A_j and B_j ($j = 0, \dots, n$) determining the characteristic position of the plastic

zone in the corresponding material are known:

$$(2.1) \quad \begin{aligned} & A_j(\bar{R}_j, a_j), \quad B_j(\underline{R}_j, b_j), \quad j = 0, \dots, n + 1, \\ & 0 = \bar{R}_0 < \dots < \bar{R}_j < \bar{R}_{j+1} < \dots < \bar{R}_{n+1} = \bar{\mathbf{R}}, \\ & 0 = \underline{R}_0 < \dots < \underline{R}_j < \underline{R}_{j+1} < \dots < \underline{R}_{n+1} = \underline{\mathbf{R}}, \end{aligned}$$

where $\bar{\mathbf{R}}$ and $\underline{\mathbf{R}}$ are radii of entry and exit of the tool, respectively.

Let $(r_a^{(j)}, z_a^{(j)}) \in \Gamma_{A_j A_{j+1}}$ and $(r_b^{(j)}, z_b^{(j)}) \in \Gamma_{B_j B_{j+1}}$ be the coordinates of an arbitrary point of metal at the entry and exit in the core ($j = 0$) or the corresponding sleeve ($j = 1, \dots, n$). Then, in view of the assumption of this section, modelling of the trajectory in the plastic zone is given by the straight line

$$(2.2) \quad z_j = \frac{1}{r_a^{(j)} - r_b^{(j)}} \left[z_a^{(j)}(r_j - r_b^{(j)}) - z_b^{(j)}(r_j - r_a^{(j)}) \right], \quad r_j \in [r_b^{(j)}, r_a^{(j)}],$$

where (r_j, z_j) are the successive positions of the point.

It is assumed that the boundaries of the plastic zone are prescribed by the following curves determined by their parametric forms:

$$(2.3) \quad \Gamma_{A_0 A_1} : \begin{cases} z_a^{(0)} = f_0(t), \\ r_a^{(0)} = \bar{R}_0 t, \end{cases}, \quad \Gamma_{B_0 B_1} : \begin{cases} z_b^{(0)} = g_0(t), \\ r_b^{(0)} = \underline{R}_0 t, \end{cases}, \quad t \in [0, 1],$$

in the core, and

$$(2.4) \quad \begin{aligned} \Gamma_{A_j A_{j+1}} : & \begin{cases} z_a^{(j)} = f_j(t), \\ r_a^{(j)} = \sqrt{\bar{R}_{j+1}^2 t^2 + \bar{R}_j^2 (1 - t^2)}, \end{cases} \\ \Gamma_{B_j B_{j+1}} : & \begin{cases} z_b^{(j)} = g_j(t), \\ r_b^{(j)} = \sqrt{\underline{R}_{j+1}^2 t^2 + \underline{R}_j^2 (1 - t^2)}, \end{cases} \end{aligned} \quad t \in [0, 1], \quad j = 1, \dots, n,$$

in the corresponding sleeves. Note that Eq. (2.2) makes sense because from the definitions (2.3) and (2.5) it follows that

$$(2.5) \quad \forall t \in [0, 1] : \quad r_b^{(j)}(t) < r_a^{(j)}(t).$$

Such description makes it possible to determine the functions f_j, g_j ($j = 0, \dots, n$). They must be monotonic functions and satisfy additional conditions concerning the geometry of the plastic zone (see Fig. 8):

$$(2.6) \quad \begin{aligned} & f_j(0) = a_j, \quad f_j(1) = a_{j+1}, \quad g_j(0) = b_j, \quad g_{j+1}(1) = b_{j+1}, \quad j = 0, \dots, n, \\ & \forall t \in [0, 1] : \quad g_j(t) > f_j(t), \quad (z_a^{(j)}(t) < z_b^{(j)}(t)). \end{aligned}$$

These restrictions correspond to the geometry of the problem presented in Fig. 8 and, on the other hand, guarantee that flow lines for different values of the parameter t (the respective straight lines) do not intersect each other.

Now following for paper [17], let us introduce auxiliary curves $\Gamma_{\lambda_j}^{(j)}$ in each material ($j = 0, \dots, n$) along which the degree of deformation is constant (equal to the value of λ_j):

$$(2.7) \quad \Gamma_{\lambda_0}^{(0)} = \left\{ (r_*^{(0)}(t), z_*^{(0)}(t)) : \left[\frac{r_a^{(0)}(t)}{r_*^{(0)}(t)} \right]^2 = \lambda_0 \right\}, \quad \lambda_0 \in [1, \bar{\lambda}_0],$$

$$\Gamma_{\lambda_j}^{(j)} = \left\{ (r_*^{(j)}(t), z_*^{(j)}(t)) : \frac{[r_a^{(j)}(1)]^2 - [r_a^{(j)}(t)]^2}{[r_*^{(j)}(1)]^2 - [r_*^{(j)}(t)]^2} = \lambda_j \right\}, \quad \lambda_j \in [1, \bar{\lambda}_j].$$

Then by direct differentiation of (2.7), the following differential equations can be found:

$$(2.8) \quad [r_*^{(0)}]_t' = \frac{r_*^{(0)}}{r_a^{(0)}} [r_a^{(0)}]_t', \quad [r_*^{(j)}]_t' = \frac{r_a^{(j)}}{\lambda_j r_*^{(j)}} [r_a^{(j)}]_t', \quad j = 1, \dots, n.$$

Their solutions are of the forms:

$$(2.9) \quad r_*^{(0)}(t) = \alpha_0 t, \quad r_*^{(j)}(t) = \sqrt{\alpha_j^2 t^2 + \alpha_{j-1}^2 (1 - t^2)}, \quad j = 1, \dots, n, \quad t \in [0, 1],$$

with some unknown constants α_j ($j = 0, \dots, n$).

Let us observe that the intermediate degree of deformation λ_j of each j -material does not depends on parameter t and, due to (2.7) and (2.9), can be calculated in the following manner:

$$(2.10) \quad \lambda_0 = \frac{\bar{R}_0^2}{\alpha_0^2}, \quad \lambda_j = \frac{\bar{R}_j^2 - \underline{R}_j^2}{\alpha_j^2 - \alpha_{j-1}^2}, \quad j = 1, \dots, n.$$

In these equations parameters α_j should belong to the corresponding intervals:

$$(2.11) \quad \alpha_j \in [\underline{R}_j, \bar{R}_j], \quad \alpha_{j|\lambda_j=1} = \bar{R}_j, \quad \alpha_{j|\lambda_j=\bar{\lambda}_j} = \underline{R}_j,$$

and can be defined by equations

$$(2.12) \quad \alpha_j = \sqrt{\frac{\bar{R}_{j+1}^2 - \underline{R}_{j+1}^2}{\bar{R}_j^2 - \underline{R}_j^2} (\alpha_{j-1}^2 - \underline{R}_j^2) + \underline{R}_{j+1}^2}, \quad j = 1, \dots, n.$$

We do not present here the arguments for choosing such a recurrent dependence between the parameters α_j and α_{j-1} . Some motivations to do this are discussed in paper [15] for $j = 1$ (the first step only). Nevertheless, one can easily check that relation (2.11) follows immediately from (2.12). Repeating the Eq. (2.12), one concludes that all parameters α_j ($j = 1, \dots, n$) depend on the unknown parameter α_0 , in fact:

$$(2.13) \quad \alpha_j = \alpha_j(\alpha_0), \quad r_*^{(j)}(t) = r_*^{(j)}(t, \alpha_0).$$

Let us note that due to Eqs. (2.3), (2.4) and the presented above definition of the auxiliary curves $\Gamma_{\lambda_j}^{(j)}$, one can prove that external boundaries of the plastic domains for each material are the limit position of the curves $\Gamma_{\lambda}^{(j)}$. Namely:

$$(2.14) \quad \Gamma_1^{(j)} = \Gamma_{A_j A_{j+1}}, \quad \Gamma_{\bar{\lambda}_j}^{(j)} = \Gamma_{B_j B_{j+1}}, \quad j = 0, 1, \dots, n.$$

Finally, the other coordinate $z_*^{(j)}(t, \alpha_0)$ of the corresponding curve $\Gamma_{\lambda}^{(j)}$ can be calculated. To do this, it is sufficient to keep in mind the straight line hypothesis:

$$(2.15) \quad z_*^{(j)}(t, \alpha_0) = \frac{1}{r_a^{(j)}(t) - r_b^{(j)}(t)} \left[z_a^{(j)}(t) (r_*^{(j)}(t, \alpha_0) - r_b^{(j)}(t)) - z_b^{(j)}(t) (r_*^{(j)}(t, \alpha_0) - r_a^{(j)}(t)) \right].$$

REMARK. Parameters t and α_0 define a consistent parametrization of each plastic domain $\Omega_j = \Omega_{A_j A_{j+1} B_{n+1} B_j}$ ($j = 0, \dots, n$) such that Eqs. (2.9) and (2.15), together with (2.3), (2.4), (2.10) and (2.12), determine maps \mathcal{M}_j :

$$(2.16) \quad \mathcal{M}_j : [0, 1] \times [\underline{R}_0, \bar{R}_0] \rightarrow \Omega_j.$$

Then the following additional condition should be true for all $t \in (0, 1)$, $\alpha_0 \in (\underline{R}_0, \bar{R}_0)$ to guarantee the existence of the inverse maps: $\mathcal{M}_j^{-1} : \Omega_j \rightarrow [0, 1] \times [\underline{R}_0, \bar{R}_0]$:

$$(2.17) \quad \begin{vmatrix} \frac{\partial}{\partial t} r_*^{(j)} & \frac{\partial}{\partial t} z_*^{(j)} \\ \frac{\partial}{\partial \alpha_0} r_*^{(j)} & \frac{\partial}{\partial \alpha_0} z_*^{(j)} \end{vmatrix} \neq 0 \Leftrightarrow \frac{\partial z_*^{(j)}}{\partial \alpha_0} \cdot \frac{\partial \alpha_0}{\partial r_*^{(j)}} \neq \frac{\partial z_*^{(j)}}{\partial t} \cdot \frac{\partial t}{\partial r_*^{(j)}}.$$

Let $\phi^{(j)}$ be the angle between the axis OZ and the trajectory of each particle of the metal defined by relation (2.2), but $\phi_N^{(j)}$ is the angle between the normal to

the curve $\Gamma_{\lambda_j}^{(j)}$ and the OZ -axis. Let us note that parameter t is constant along the trajectory of any particle, but the next parameter α_0 is constant along the curves $\Gamma_{\lambda_j}^{(j)}$. Hence, the introduced angles $\phi^{(j)} = \phi(t)$ and $\phi_N^{(j)} = \phi_N(t, \alpha_0)$ are defined from the relations:

$$(2.18) \quad \operatorname{tg} \phi^{(j)} = \frac{\partial r_*^{(j)}}{\partial \alpha_0} \cdot \frac{\partial \alpha_0}{\partial z_*^{(j)}} = \frac{r_a^{(j)}(t) - r_b^{(j)}(t)}{z_a^{(j)}(t) - z_b^{(j)}(t)}, \quad t \in [0, 1],$$

$$(2.19) \quad \operatorname{tg} \phi_N^{(j)} = -\frac{\partial z_*^{(j)}}{\partial t} \cdot \frac{\partial t}{\partial r_*^{(j)}}, \quad t \in [0, 1], \quad \alpha_0 \in [\underline{R}_0, \overline{R}_0].$$

Using these angles, condition (2.17) can be rewritten in an equivalent form:

$$(2.20) \quad \operatorname{tg} \phi_N^{(j)} \neq -\operatorname{ctg} \phi^{(j)} \Leftrightarrow |\phi^{(j)} - \phi_N^{(j)}| \neq \pi/2, \quad t \in (0, 1), \quad \alpha_0 \in (\underline{R}_0, \overline{R}_0).$$

Following the paper [20], values of velocities in each component can be found due to incompressibility of the materials:

$$(2.21) \quad V^{(j)}(t, \alpha_0) = \lambda_j(\alpha_0) V_{0j} \frac{\cos \phi_N^{(j)}(t, \alpha_0)}{\cos[\phi^{(j)}(t) - \phi_N^{(j)}(t, \alpha_0)]},$$

$$t \in [0, 1], \quad \alpha_0 \in [\underline{R}_0, \overline{R}_0],$$

but directions of the velocities $V^{(j)}$ are determined by the mentioned angle $\phi^{(j)}$ in the corresponding point.

Then the axial and radial components of the velocities are

$$(2.22) \quad V_r^{(j)} = -V^{(j)} \sin \phi^{(j)}, \quad V_z^{(j)} = -V^{(j)} \cos \phi^{(j)},$$

where the direction of the velocity vectors has been taken into account.

Now we show that the condition (2.17) and, consequently, the condition (2.20) is satisfied in the case under consideration.

To this end, let us write coordinate $z_*^{(j)}(t, \alpha_0)$ (see Eq. (2.15)) as a function of variables t and r_* (the last one is, in turn a function of t and α_0), so that

$$z_*^{(j)}(t, r_*) = z_{**}^{(j)}(t, r_*^{(j)}(t, \alpha_0)) = z_*^{(j)}(t, \alpha_0).$$

Then condition (2.17) is rewritten in the following form:

$$\frac{\partial z_*^{(j)}}{\partial \alpha_0} \cdot \frac{\partial \alpha_0}{\partial r_*^{(j)}} \neq \frac{\partial z_{**}^{(j)}}{\partial t} \cdot \frac{\partial t}{\partial r_*^{(j)}} + \frac{\partial z_{**}^{(j)}}{\partial r_*^{(j)}}.$$

From Eq. (2.15) it follows that the left-hand side of the last inequality is identical with the second term of the right-hand side. Hence, condition (2.20) is in our case is equivalent to the following one:

$$(2.23) \quad \frac{\partial z_{**}^{(j)}}{\partial t} \cdot \frac{\partial t}{\partial r_*^{(j)}} \neq 0 \Rightarrow \frac{\partial z_{**}^{(j)}}{\partial t} \neq 0, \quad t \in (0, 1), \quad \alpha_0 \in (\underline{R}_0, \overline{R}_0),$$

here the relations (2.3) and (2.4) have been taken into account.

After some calculations, the last inequality can be rewritten in the form:

$$\begin{aligned} (r_*^{(j)} - r_b^{(j)}) \{ [r_a^{(j)}]' + \operatorname{tg} \phi^{(j)} [z_a^{(j)}]' \} + (r_a^{(j)} - r_*^{(j)}) \{ [r_b^{(j)}]' \\ + \operatorname{tg} \phi^{(j)} [z_b^{(j)}]' \} \neq 0. \end{aligned}$$

Finally, it remains to note that the terms in parentheses are always non-negative, so we can obtain the following restriction for functions f_j and g_j determining boundaries $\Gamma_{A_j A_{j+1}}$ and $\Gamma_{B_j B_{j+1}}$ of the corresponding domain (see Eqs. (2.3) and (2.4)):

$$(2.24) \quad \forall t \in (0, 1]: \quad \left(1 + \operatorname{tg} \phi^{(j)} [z_a^{(j)}]' / [r_a^{(j)}]' \right) \cdot \left(1 + \operatorname{tg} \phi^{(j)} [z_b^{(j)}]' / [r_b^{(j)}]' \right) > 0.$$

Let us note that condition (2.24) is essentially simpler than condition (2.17), however these two conditions are equivalent. For example, if $[z_a^{(j)}]' \geq 0$ and $[z_b^{(j)}]' \geq 0$ then condition (2.24) is satisfied.

Let us now present the formulae for all velocity discontinuities. Thus, along the bimaterial interfaces we obtain:

$$\begin{aligned} (2.25) \quad \Delta V_{|\Gamma_{A_j B_j}}(\alpha_0) &= [V^{(j)}(0, \alpha_0) - V^{(j-1)}(1, \alpha_0)] \\ &= -\frac{1}{\cos \phi_j} \left(\frac{V_{0j} \lambda_j(\alpha_0)}{1 + \operatorname{tg} \phi_j \operatorname{tg} \phi_N^{(j)}(0, \alpha_0)} - \frac{V_{0(j-1)} \lambda_{j-1}(\alpha_0)}{1 + \operatorname{tg} \phi_j \operatorname{tg} \phi_N^{(j-1)}(1, \alpha_0)} \right), \\ &\quad \phi_j = \phi^{(j)}(0) = \phi^{(j-1)}(1), \quad j = 1, \dots, n. \end{aligned}$$

but along the dead zone boundary $A_{n+1} B_{n+1}$ the following relation holds true:

$$(2.26) \quad \Delta V_{|\Gamma_{A_{n+1} B_{n+1}}}(\alpha_0) = \frac{V_{0(n+1)} \lambda_n(\alpha_0)}{\cos \phi_n [1 + \operatorname{tg} \phi_n \operatorname{tg} \phi_N^{(n)}(1, \alpha_0)]}.$$

Now let us calculate the velocity discontinuities at the entry of the plastic zone ($n = 0, \dots, n$):

$$\begin{aligned}
 (2.27) \quad \Delta V_{z|\Gamma_{A_j A_{j+1}}} &= -V_{0j} \frac{\cos \phi^{(j)}(t) \cos \phi_N^{(j)}(t, \bar{R}_0)}{\cos[\phi^{(j)}(t) - \phi_N^{(j)}(t, \bar{R}_0)]} + V_{0j} \\
 &= V_{0j} \frac{\sin \phi^{(j)}(t) \sin \phi_N^{(j)}(t, \bar{R}_0)}{\cos[\phi^{(j)}(t) - \phi_N^{(j)}(t, \bar{R}_0)]},
 \end{aligned}$$

$$\begin{aligned}
 (2.28) \quad \Delta V_{r|\Gamma_{A_j A_{j+1}}} &= -V_{0j} \frac{\sin \phi^{(j)}(t) \cos \phi_N^{(j)}(t, \bar{R}_0)}{\cos[\phi^{(j)}(t) - \phi_N^{(j)}(t, \bar{R}_0)]}, \quad |\overline{\Delta V}|_{|\Gamma_{A_j A_{j+1}}} \\
 &= V_{0j} \frac{\sin \phi^{(j)}(t)}{\cos[\phi^{(j)}(t) - \phi_N^{(j)}(t, \bar{R}_0)]}.
 \end{aligned}$$

At the exit boundary of the plastic zone, the respective equations hold:

$$\begin{aligned}
 (2.29) \quad \Delta V_{z|\Gamma_{B_j B_{j+1}}} &= V_{0j} \bar{\lambda}_j \frac{\cos \phi^{(j)}(t) \cos \phi_N^{(j)}(t, \underline{R}_0)}{\cos[\phi^{(j)}(t) - \phi_N^{(j)}(t, \underline{R}_0)]} - V_{fj} \\
 &= -V_{fj} \frac{\sin \phi^{(j)}(t) \sin \phi_N^{(j)}(t, \underline{R}_0)}{\cos[\phi^{(j)}(t) - \phi_N^{(j)}(t, \underline{R}_0)]},
 \end{aligned}$$

$$\begin{aligned}
 (2.30) \quad \Delta V_{r|\Gamma_{B_j B_{j+1}}} &= V_{fj} \frac{\sin \phi^{(j)}(t) \cos \phi_N^{(j)}(t, \underline{R}_0)}{\cos[\phi^{(j)}(t) - \phi_N^{(j)}(t, \underline{R}_0)]}, \quad |\overline{\Delta V}|_{|\Gamma_{B_j B_{j+1}}} \\
 &= V_{fj} \frac{\sin \phi^{(j)}(t)}{\cos[\phi^{(j)}(t) - \phi_N^{(j)}(t, \underline{R}_0)]}.
 \end{aligned}$$

In Eqs. (2.29) and (2.30), the obvious relation is used:

$$(2.31) \quad V_{fj} = \bar{\lambda}_j V_{0j}.$$

3. MODEL 2. SMOOTH FLOW LINES

In this section, the other equation describing the flow lines in plastic zone is considered (see Fig. 9).

Namely, the following equation for the flow line, proposed first in the paper [18] for bimaterial extrusion, is applied instead of (2.2):

$$(3.1) \quad z_j = z_a^{(j)} - \frac{z_a^{(j)} - z_b^{(j)}}{\pi} \arccos \left[\frac{2r_j - r_a^{(j)} - r_b^{(j)}}{r_a^{(j)} - r_b^{(j)}} \right], \quad r_j \in [r_b^{(j)}, r_a^{(j)}],$$

where (r_j, z_j) are as usual the successive positions of the points in plastic domain.

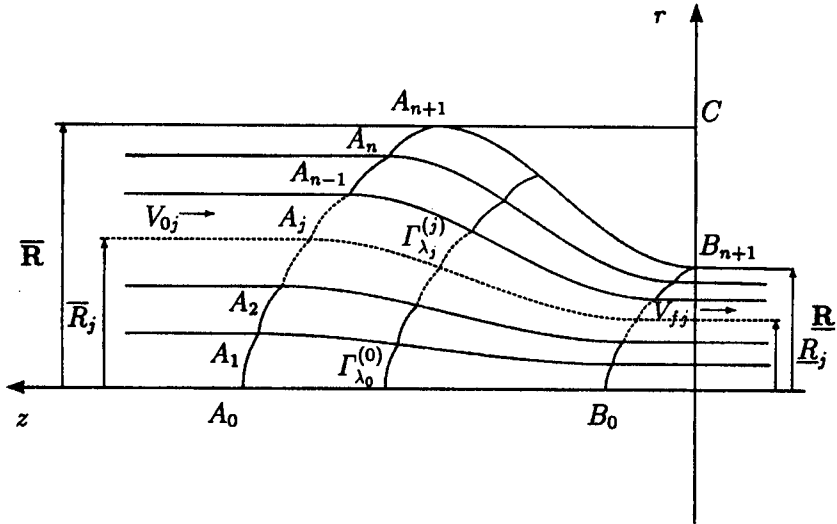


FIG. 9. Multimetal extrusion with smooth flow lines.

Equations (2.1) – (2.14) remain to be true for this velocity field without any changes. Equation (2.15) describing the second coordinate of the auxiliary curves $\Gamma_{\lambda_j}^{(j)}$, follows immediately from Eq. (3.1) in the form:

$$(3.2) \quad z_*^{(j)}(t, \alpha_0) = z_a^{(j)}(t) - \frac{z_a^{(j)}(t) - z_b^{(j)}(t)}{\pi} \arccos \left[\frac{2r_*^{(j)}(t, \alpha_0) - r_a^{(j)}(t) - r_b^{(j)}(t)}{r_a^{(j)}(t) - r_b^{(j)}(t)} \right],$$

$$t \in [0, 1], \quad \alpha_0 \in [\underline{R}_0, \bar{R}_0].$$

Let $\phi^{(j)}$ and $\phi_N^{(j)}$ be the angles determined above. Then Eq. (2.19) still holds true, but the angle $\phi^{(j)} = \phi^{(j)}(t, \alpha_0)$ is defined by the other equation than (2.18):

$$(3.3) \quad \text{tg } \phi^{(j)} = \frac{\pi \sqrt{(r_a^{(j)}(t) - r_*^{(j)}(t, \alpha_0))(r_*^{(j)}(t, \alpha_0) - r_b^{(j)}(t))}}{z_a^{(j)}(t) - z_b^{(j)}(t)},$$

$$t \in [0, 1], \quad \alpha_0 \in [\underline{R}_0, \bar{R}_0].$$

From this equation it is easily seen that

$$(3.4) \quad \phi^{(j)}|_{\Gamma_{A_j, A_{j+1}}} = \phi^{(j)}(t, \bar{R}_0) = 0, \quad \phi^{(j)}|_{\Gamma_{B_j, B_{j+1}}} = \phi^{(j)}(t, \underline{R}_0) = 0,$$

$$j = 0, \dots, n.$$

Equations (2.21), (2.22), (2.25) – (2.31) still hold true if in the corresponding formulae, the angles $\phi^{(j)}(t)$ are replaced by $\phi^{(j)}(t, \alpha_0)$, and, consequently, the angle ϕ_j by $\phi_j(\alpha_0) = \phi^{(j)}(0, \alpha_0) = \phi^{(j-1)}(1, \alpha_0)$.

The additional condition should be considered in the general form (2.17) or, what is equivalent, in form (2.20). Moreover, repeating the same line of reasoning as above, we arrive at condition (2.20), where function $z_{**}^{(j)}$ is defined by Eq. (3.2) if function $r_*^{(j)}(t, \alpha_0)$ is considered to be constant. Then the corresponding condition is rewritten in the form:

$$(3.5) \quad [z_a^{(j)}]' - \frac{1}{\pi} \left([z_a^{(j)}]' - [z_b^{(j)}]' \right) \arccos \left[\frac{2r_* - r_a^{(j)} - r_b^{(j)}}{r_a^{(j)} - r_b^{(j)}} \right] - \left([r_a^{(j)}]' - [r_b^{(j)}]' \right) \frac{z_a^{(j)} - z_b^{(j)}}{r_a^{(j)} - r_b^{(j)}} \sqrt{\frac{r_* - r_b^{(j)}}{r_a^{(j)} - r_*}} \neq 0, \quad t \in [0, 1],$$

$$r_* \in [r_b^{(j)}, r_a^{(j)}].$$

To simplify the last condition, it is sufficient to investigate the derivative of the left-hand side of the inequality with respect to variable r_* only. It is equal to the following expression

$$(3.6) \quad -\frac{1}{\pi} \left([z_a^{(j)}]' - [z_b^{(j)}]' \right) - \frac{1}{2(r_a^{(j)} - r_*)} \left(z_a^{(j)} - z_b^{(j)} \right) \left([r_a^{(j)}]' - [r_b^{(j)}]' \right),$$

with the accuracy up to a positive multiplier. Hence, the left-hand side of (3.5) can have only one extremal point in the interval $[r_b^{(j)}, r_a^{(j)}]$. Then the general condition (3.5) for functions f_j and g_j (see (2.4) and (2.6)) is easily verified numerically.

Some simple necessary (not sufficient!) conditions can be also obtained. To do this, the values of the left-hand side of inequality (3.5) should be calculated at three characteristic points: $r_* = r_b^{(j)}$, $r_* = (r_a^{(j)} + r_b^{(j)})/2$ and $r_* = r_a^{(j)}$, which have to be of the same sign for all $t \in (0, 1)$:

$$(3.7) \quad \begin{aligned} & z_b^{(j)}(t) > 0 \quad (< 0), \quad \left([r_a^{(j)}]' - [r_b^{(j)}]' \right) > 0 \quad (< 0), \\ & \left([z_a^{(j)}]' + [z_b^{(j)}]' \right) - 2 \left([r_a^{(j)}]' - [r_b^{(j)}]' \right) \frac{z_a^{(j)} - z_b^{(j)}}{r_a^{(j)} - r_b^{(j)}} > 0 \quad (< 0). \end{aligned}$$

Some of these conditions can be sufficient conditions, too. For example, if the following inequality

$$\forall t \in (0, 1) : \left([z_a^{(j)}]' - [z_b^{(j)}]' \right) \cdot \left([r_a^{(j)}]' - [r_b^{(j)}]' \right) < 0,$$

is satisfied in the expression (3.6), then the derivative has no zero point in the interval $r_* \in [r_b^{(j)}, r_a^{(j)}]$ and the left-hand side of condition (3.5) is strictly monotonic (see (2.5) and (2.6)). Then only one of the conditions (3.7) should be considered and this condition in the corresponding end points of interval $r_* \in [r_b^{(j)}, r_a^{(j)}]$ is equivalent to the general condition (2.20).

In conclusion let us note that in the case of curvilinear flow line, there are no velocity discontinuities along boundaries $\Gamma_{A_j A_{j+1}}$ and $\Gamma_{B_j B_{j+1}}$. This fact can be easily checked by substituting relations (3.4) into Eqs. (2.27) – (2.30).

4. DISCUSSIONS AND CONCLUSIONS

Using the models of velocity fields presented above it is possible to calculate the strain-rate tensor and then, by the Saint-Venant – Levy – Mises hypotheses, to find deviatoric part of the stress tensor. The numerical algorithm necessary to evaluate components of the strain-rate tensor at an arbitrary point in each material can be taken from the paper [18].

On the other hand, application of the proposed model to the upper bound method makes it possible to define an optimal design of multi-metal extrusion. Let us note that, in fact, only geometrical parameters determined for the initial or final stage of the process can be chosen in an arbitrary way.

In the first case, the geometrical parameters: \bar{R}_j , \underline{R}_{n+1} , and velocities V_{0j} ($j = 0, \dots, n$) are assumed to be known as well as all mechanical parameters: Y_j - yield stress of each material, and m_j - friction parameter determining friction between materials $j - 1$ and j . Then the corresponding problem is to define all the expected geometrical parameters at the exit of the plastic zone: \underline{R}_j ($j = 0, \dots, n$) under restrictions (2.2), (2.20) and some additional restrictions which deal with internal parameters of the process (strain hardening, fracture). In fact, the extrusion problem for $n + 1$ materials (a core and n sleeves) is an optimization problem with at least $N \geq 3n + 4$ optimization parameters. Thus, if the simplest case is considered (straight lines $\Gamma_{A_j A_{j+1}}$ and $\Gamma_{B_j B_{j+1}}$ and there is no internal mechanical parameter), then $N = 3n + 4$. Let us note that in this case all functions $f_j(t)$ and $g_j(t)$ are monotonic and satisfy conditions (2.4) – (2.7). In such the case, as optimization parameters we have: a_j ($j = 0, \dots, n + 1$); b_j ($j = 0, \dots, n, b_{n+1} = 0$); \underline{R}_j ($j = 0, \dots, n$). What is important to note is that velocities V_{fj} ($j = 0, \dots, n$) are not the optimization parameters, because they

are easily calculated from relations (2.31) once the parameters mentioned above have been defined. However, in the author's opinion, such minimal optimization ($N = 3n + 4$) cannot be considered as an appropriate one. This is because, from the experimental results one can see that lines $\Gamma_{A_j A_{j+1}}$ and $\Gamma_{B_j B_{j+1}}$ are not straight lines, in general. The other reason is that derivatives of functions $f_j(t)$ and $g_j(t)$ are always constant in this case. As a simple inconsistency of this approach we can note that the curve $\Gamma_{A_n A_{n+1}}$ can not be tangent to the tool boundary $A_{n+1}C$ as well as the curve $\Gamma_{B_n B_{n+1}}$ can not be perpendicular to tool boundary CB_{n+1} at all. However, exactly such a geometry is often observed in experiments [15, 16, 19].

The other problem for multi-material extrusion which can be considered is the inversed problem when all entry parameters of the problem should be calculated in order to obtain some necessary final product.

Finally, let us note that the condition (2.20) should be checked only at the first step of the optimization procedure. In fact, if values of the optimization parameters are near the point where condition (2.20) is not satisfied, the corresponding velocities and, consequently, strain rate tensor components take large values due to condition (2.20) and Eq. (2.21). As a result, the next step point will be far away from the dangerous point.

Both the models presented here are based on assumptions taking into account real character of the plastic flow of various metals under extrusion. Differentiation of the flow of these materials are confirmed under presented test conditions (see Figs. 2 – 7). Considering advantages and disadvantages of the presented models, it may be stated that the Model I is simpler than the Model II, but in the first model the displacement discontinuity appears at the entry and the exit of the plastic zone. Nevertheless, both of them may be used to determine the multi-material flow under such mode of plastic deformation.

ACKNOWLEDGEMENTS

One of the authors (Gennady S. Mishuris) is an Alexander von Humboldt Fellow from July 1999.

REFERENCES

1. J.L. ALCARAZ, J.M. MARTINEZ-ESNAOLA and J. GIL-SEVILLANO, *An analytical approach to the stress field in the extrusion of bimetallic tubes*, Int. J. Solids Structures, **33**, 14, 2075–2093, 1996.
2. J.L. ALCARAZ and J. GIL-SEVILLANO, *An analysis of the extrusion of bimetallic tubes by numerical simulation*, Int. J. Mech. Sci, **38**, 2, 157–173, 1996.

3. J.L. ALCARAZ and J. GIL-SEVILLANO, *Safety maps in bimetallic extrusions*, Jour. Mat. Proc. Techn, **60**, 133–140, 1996.
4. B. AVITZUR, R. WU, S. TALBOT and Y.T. CHOU, *Criterion for the prevention of core fracture during extrusion of bimetal rods*, ASME J. Engng. Ind., **104**, 293–304, 1982.
5. B. AVITZUR, *Handbook of metal-forming processes*, Wiley, New York 1983.
6. T.Z. BLAZYŃSKI [Ed.], *Plasticity and modern metal-forming technology*, Elsevier, London 1989.
7. M.S. GILDENDORN, *Fundamental theory of simultaneous extrusion of metals and alloys of various mechanical features* [in Russian], Mietallurgija, Moskwa 1981.
8. W. JOHNSON and P.B. MELLOR, *Engineering plasticity*, Ellis Horwood Ltd., Chichester 1986.
9. W.K. KOROL and M.S. GILDERDORN, *Technological fundamentals of production of multi-layer metals* [in Russian], Mietallurgija, Moskwa 1970.
10. K. LAUE and H. STENGER, *Extrusion*, American Society for Metals, Metals Park, Ohio 1981.
11. H. LIPPMANN and H. ABSCHÄTZEN, *Oberer und unterer Schranken für Umformungsleitungen und -Kräfte, besonders bei Strangpressen*, Verlag Stahleisen, Düsseldorf 1966. Naturwissenschaften, **72**, 633–639.
12. F. MAVUNDA and J. ZASADZIŃSKI, *Dead zones in the process of direct extrusion of metals*, Archiwum Hutnictwa, **28**, 3, 359–403, 1983.
13. K. OSAKADA, M. LIMB and P.B. MELLOR, *Int. J. Mech. Sci.*, **15**, 291–307, 1973.
14. S.R. REID [Ed.], *Metal forming and impact mechanics*, Pergamon, Oxford 1985.
15. R.E. ŚLIWA, *A test determining the ability of different materials to undergo simultaneous plastic deformation to produce metal composites*, Mat. Sci. Engng., **A 135**, 259–265, 1991.
16. R.E. ŚLIWA, *Plastic zones in the extrusion of metal composites*, Jour. Mat. Proc. Techn., **67**, 29–35, 1997.
17. R.E. ŚLIWA and G. MISHURIS, *Modelling the plastic flow of composite materials in the extrusion process*, Engng. Trans, **45**, 2, 275–293, 1997.
18. R.E. ŚLIWA and G. MISHURIS, *Modified flow field in the extrusion of bimetallic systems*, Engng. Trans., **47**, 2, 203–215, 1999.
19. R.E. ŚLIWA, *Plastic zones in extrusion of longitudinally oriented metal composites*, Proc. Conf. Mechanics of Solids and Materials Engineering, Singapore'95, **A**, 179–184, 1995.
20. H. TOKUNO and K. IKEDA, *Analysis of deformation in extrusion of composite rods*, Jour. Mat. Proc. Techn, **26**, 323–335, 1991.
21. D.Y. YANG, H.S. KIM, C.M. LEE, C.H. HAN, *Int. J. Mech. Sci.*, **32**, 2, 115–127, 1990.
22. D.Y. YANG, H.S. KIM, C.M. LEE, *CIRP Ann.*, **36**, 1, 169–172, 1997.